RSC Advances

PAPER

View Article Online
View Journal | View Issue

Cite this: *RSC Adv.*, 2022, **12**, 7453

Graphene oxide based crosslinker for simultaneous enhancement of mechanical toughness and self-healing capability of conventional hydrogels†

Md. Mahamudul Hasan Rumon, ‡[a] Stephen Don Sarkar, ‡[a] Md. Mosfeq Uddin, [a] Md. Mahbub Alam, [a] Sadia Nazneen Karobi, [b] Aruna Ayfar, [a] Md. Shafiul Azam *[a] and Chanchal Kumar Roy *[a]

Extraordinary self-healing efficiency is rarely observed in mechanically strong hydrogels, which often limits the applications of hydrogels in biomedical engineering. We have presented an approach to utilize a special type of graphene oxide-based crosslinker (GOBC) for the simultaneous improvement of toughness and self-healing properties of conventional hydrogels. The GOBC has been prepared from graphene oxide (GO) by surface oxidation and further introduction of vinyl groups. It has been designed in such a way that the crosslinker is able to form both covalent bonds and noncovalent interactions with the polymer chains of hydrogels. To demonstrate the efficacy of GOBC, it was incorporated in a conventional polyacrylamide (PAM) and polyacrylic acid (PAA) hydrogel matrix, and the mechanical and self-healing properties of the prepared hydrogels were investigated. In PAM-GOBC hydrogels, it has been observed that the mechanical properties such as tensile strength, Young's modulus, and toughness are significantly improved by the incorporation of GOBC without compromising the self-healing efficiency. The PAM-GOBC hydrogel with a modulus of about 0.446 MPa exhibited about 70% stress healing efficiency after 40 h. Whereas, under the same conditions a PAM hydrogel with commonly used crosslinker *N*,*N*′-methylene-bis(acrylamide) of approximately the same modulus demonstrated no self-healing at all. Similar improvement of self-healing properties and toughness in PAA-GOBC hydrogel has also been observed which demonstrated the universality of the crosslinker. This crosslinker-based approach to improve the self-healing properties is expected to offer the possibility of the application of commonly used hydrogels in many different sectors, particularly in developing artificial tissues.

Received 8th January 2022
Accepted 1st March 2022

DOI: 10.1039/d2ra00122e

rsc.li/rsc-advances

1. Introduction

Hydrogels have attracted significant attention for diverse applications owing to their biocompatibility, water uptake, and responsive properties.[1] Especially in biomedical engineering, they have been used for the development of soft robotics,[2] bio-sensors,[3–5] drug reservoirs,[6,7] bio-separators,[8] bio-catalysts,[9,10] *etc.* Artificial organs such as the ear, heart, cartilage, ligament, *etc.* are in their early stages of development from hydrogels.[11–13] High mechanical toughness, long stretchability, strong adhesiveness, strain softening/stiffening and good self-healing capability are some of the key features for the fabrication of artificial tissues.[14–17] For the advanced uses of hydrogels in materials science such as soft-robotics and flexible electronics, the hydrogels are also required to be very tough with high self-healing ability.[18] However, combinations of these properties have been rarely achieved in hydrogels so far. The leading problem associated with the properties of hydrogels is that the improvement of the mechanical strongness often results in the weakening of self-healing properties.[19] There is a common trade-off between the modulus of hydrogels and self-healing properties.[18–21] Several efforts have been directed towards designing synthetic hydrogels to attain the unique combination of mechanical toughness and self-healing properties by introducing special types of reversible nature of physical bonds in polymeric networks of hydrogels,[22] such as covalent bonds,[23] ionic bonds,[24] hydrogen bonds,[25] hydrophobic interactions,[26,27] host–guest interactions,[28] π–π stacking,[29] *etc.* The most notable contribution in the development of tough hydrogels with self-healing capabilities is the polyampholyte hydrogels.[30,31] About 90% of healing efficiency with high toughness was obtained in the polyampholyte hydrogels. The presence of ionic bonds of different strengths was introduced by utilizing cationic and anionic monomers. The strong irreversible covalent bonds enhanced the mechanical properties whereas weak reversible

[a]*Bangladesh University of Engineering and Technology (BUET), Dhaka-1000, Bangladesh. E-mail: azam@ualberta.ca; ckroy@chem.buet.ac.bd*

[b]*Independent University Bangladesh (IUB), Dhaka-1229, Bangladesh*

† Electronic supplementary information (ESI) available. See DOI: 10.1039/d2ra00122e

‡ Authors have equal contribution.

physical bonds improved the self-healing properties of the hydrogels.

Most of the approaches for the simultaneous improvement of mechanical toughness and self-healing were very specific, dominated by the choice of special types of polymers and dedicated to specific types of polymeric hydrogels. Improvements of conventional and regularly used hydrogels like polyacrylamide (PAM) and polyacrylic acid (PAA) hydrogels have received comparatively less attention in this regard. The core limitation associated with the reported approaches is the absence of a general strategy to be applied for most polymeric hydrogel networks. Here, the crosslinker-based approach is appeared as the effective strategy to address this issue. Several types of crosslinkers have already been developed in recent years. For instance, Fan *et al.* converted tannic acid into a crosslinker and applied it in PAM and polyvinyl alcohol hydrogels.[32] Significant improvement in toughness, adhesiveness, and swelling resistance was observed in their study. However, only about 40% self-healing efficiency was evident for PAM-tannic acid hydrogels. Desired improvement in self-healing property may not be obtained due to the presence of inherent low crosslinking sites and weak bonding interactions with conventional polymeric networks of the hydrogels. Therefore, a new crosslinker with abundant crosslinking sites for establishing numerous bonding interactions with most of the polymer chains could be the preference to solve this problem.

The GO is one of the promising crosslinking materials to enhance the functionality of nanocomposite hydrogels.[33] Recently, a facile route to prepare a novel functionalized graphene oxide-based crosslinker (GOBC) has been reported in one of the research works.[34] This special crosslinker contains anchored acrylate groups in addition to surface functional species. The 2D surface of GO nanosheets contains a good abundance of oxygen-containing functional groups *e.g.*, carboxyl, epoxide, and hydroxyl groups. Therefore, various dynamic reversible physical bonds including hydrogen bonds, dipole–dipole interactions, ionic interactions, *etc.* can be formed with different polymer chains. Additionally, the presence of acrylate groups on the GOBC surface offers the ability of the crosslinker to covalently bond with a large number of monomers used for the preparation of different conventional hydrogels. Significant improvements in both toughness and Young's modulus were achieved in PAA-GOBC hydrogels compared to the conventional *N*,*N*′-methylene-bis(acrylamide) (MBA) crosslinked PAA hydrogels. For these reasons, GOBC can be an excellent choice as a crosslinker for simultaneous improvement of mechanical properties and self-healing behavior of different hydrogels.

In this study, we have prepared GOBC from GO, and incorporated it into conventional PAM and PAA matrices to prepare nanocomposite hydrogels. The mechanical properties and self-healing capability of these GOBC crosslinked hydrogels have been investigated for various compositions of GOBC. The obtained experimental results have been analyzed and discussed in detail to evaluate the effect of GOBC on the self-healing efficiency and toughness of the prepared hydrogels.

2. Experimental

2.1 Chemicals and materials

Ultra-pure graphite flakes (assay 99% carbon basis), *N*-hydroxysuccinimide (NHS), *N*-(3-dimethylaminopropyl)-*N*′-ethylcarbodiimide hydrochloride (EDC), 2-aminoethyl methacrylate hydrochloride (AEM), *N*,*N*′-methylene-bis(acrylamide) (MBA), hydrogen peroxide (H_2O_2) and cellulose membrane dialysis tube (average diameter 16 mm and molecular weight cut off 14 kDa) were purchased from Sigma Aldrich. Nitric acid (HNO_3), hydrochloric acid (HCl), sulfuric acid (H_2SO_4), potassium permanganate ($KMnO_4$), sodium nitrate ($NaNO_3$), sodium hydroxide (NaOH), chloroacetic acid ($ClCH_2COOH$), acrylamide (AM), and potassium persulfate (KPS) were obtained from Merck, Germany. Acrylic acid (AA) was purchased from Loba Chemie, India. All the chemicals were analytical reagent grade and used as received.

2.2 Preparation of GOBC

The conversion of GOBC from GO nanosheets was conducted following Hummers' method.[35,36] For GO preparation, 1 g of previously oxidized graphite flakes was mixed with 1.03 g of $NaNO_3$ and 62 g of concentrated H_2SO_4 in a round-bottom flux at a temperature below 20 °C. 4.5 g of $KMnO_4$ was slowly added to the mixture with continuous stirring and left for two days at room temperature to complete the reaction. The reaction was then quenched by adding deionized (DI) water. The product was centrifuged and washed with DI water several times, and dried in a vacuum oven at 60 °C to obtain GO nanosheets. Then carboxylated GO (CGO) was synthesized from the prepared GO nanosheets by oxidizing with chloroacetic acid under strong basic conditions. 10 mL of an aqueous suspension of GO nanosheets (2 mg mL^{-1}) was sonicated with 12 g of NaOH and 10 g of $ClCH_2COOH$ for 2 h. The obtained product, CGO, was centrifuged and washed with DI water to remove unwanted ionic impurities. Finally, GOBC was prepared by the EDC coupling reaction of CGO with AEM.[34] Primarily, 24 mg of EDC and 20 mg of NHS were added to a 10 mL aqueous suspension of CGO (2 mg mL^{-1}) and left under continuous stirring for 2 h in an ice bath. Then 180 mg of AEM was added to the mixture and stirred overnight at room temperature. The resulting GOBC suspension was centrifuged and dialyzed against DI water at room temperature for 3 days to remove impurities. The obtained GOBC was employed as a crosslinker for the preparation of PAM and PAA hydrogels.

2.3 Preparation of PAM-GOBC and PAA-GOBC hydrogels

The PAM-GOBC nanocomposite hydrogels containing different compositions of GOBC were prepared by free radical polymerization of AM monomer in presence of GOBC using KPS as initiator. The concentration of AM monomer was kept at 5 M for all PAM hydrogels. AM monomer, GOBC (in a mass% with respect to AM), and KPS (0.01 mole% with respect to AM) were mixed in a beaker and DI water was added to achieve 5 M AM monomer concentration. The mixture was transferred to a glass mold consisting of two parallel glass plates separated by a 2 mm

silicon spacer. The glass mold containing the reaction was then heated for 8 h at 43 °C in an inert atmosphere for polymerization reaction to obtain PAM-GOBC hydrogel. PAM hydrogels containing MBA, and GO crosslinkers (added in a mass% with respect to monomer) were also prepared following the same procedure. To investigate the contribution of GOBC in the self-healing capability of PAA hydrogels, GOBC incorporated PAA hydrogel was prepared following the similar process keeping the AA monomer concentration at 5 M. The prepared hydrogels were collected from the mold to study the mechanical properties, swelling behavior, and self-healing capability.

2.4 Spectroscopic characterizations

The UV/Vis absorption spectra of GO, CGO, and GOBC dispersions were recorded using a UV/Visible spectrophotometer (Shimadzu-1800, Japan). The vacuum-dried samples of GO, CGO, and GOBC were used for Fourier transform infrared spectroscopic (FT-IR) analysis. A very small amount of prepared materials were mixed with KBr powder for making pellets. FT-IR spectra were recorded in the range of 4000–400 cm^{-1} in an FT-IR-8400 instrument (Shimadzu, Japan).

2.5 Mechanical tests

The tensile tests of the prepared hydrogels were carried out using a universal testing machine (Test Resources, 100P250-12 System, USA). The hydrogels prepared with 2 mm thickness were cut into rectangular shapes with about 10 mm length and about 4 mm width for tensile measurements. The tensile tests were conducted at a crosshead speed of 100 mm min^{-1}. The stress of the samples was calculated by using the equation $\sigma = F/A$, where F is the load and A is the cross-sectional area of the specimen. The strain was measured from the elongation of sample length (Δl) and initial length (l_o) following the equation $\varepsilon = \Delta l/l_o$. The initial linear region of the stress–strain curves was used to calculate Young's modulus. The toughness was calculated by integrating the area underneath the stress–strain curve of each specimen before fracture.

2.6 Swelling ratio measurements

The prepared hydrogels with 2 mm thickness were cut into pieces of small rectangular shapes (around 3 mm length and 5 mm width) maintaining approximately similar weights to investigate swelling behavior. The pieces were immersed into separate containers of 500 mL DI water and left for swelling at room temperature for various time durations. The swelling ratio of the samples was calculated using the following equation:[37,38]

$$SR = (W_t - W_d)/W_d$$

where W_t is the weight of the swollen hydrogel at a certain time and W_d is the weight of the corresponding dry hydrogel.

2.7 Self-healing measurement

The hydrogel samples were cut and then joined to investigate the self-healing behavior of the prepared hydrogels. The rectangular-shaped hydrogels (length 10 mm × width 4 mm) were cut into two parts (cut-in-half) by a sharp blade. Then, the separated hydrogels were brought in contact as soon as possible at the same cut place and stored in an airtight box to prevent evaporation during the healing process. After various time periods, tensile tests of the healed hydrogel samples were performed at 100 mm min^{-1} velocity to inspect self-healing properties. The fracture stress (σ), and fracture strain (ε) of the healed hydrogels were also recorded. The tensile test of the same type of uncut or original sample was performed separately. The different mechanical parameters of healed and original samples were compared to evaluate the healing efficiency. The stress healing efficiency (η_σ) was calculated using the equation, $\eta_\sigma = \sigma_{healed}/\sigma_{original} \times 100\%$, and the equation, $\eta_\varepsilon = \varepsilon_{healed}/\varepsilon_{original} \times 100\%$ was used for the calculation of strain healing efficiency (η_ε). Here the fracture stresses of the healed sample and original sample were considered as σ_{healed} and $\sigma_{original}$ respectively. The ε_{healed} and $\varepsilon_{original}$ represent the fracture strain of the healed sample and original respectively.

3. Results and discussion

3.1 Characterization of GO, CGO, and GOBC

The successful conversion of GOBC from GO nanosheets was investigated by UV-Vis and FT-IR spectroscopic analysis. For UV-Vis absorption analysis, the aqueous suspensions of GO, CGO, and GOBC were prepared in an equal density (0.2 mg mL^{-1}) and their absorption spectra were recorded. The absorption spectra of GO, CGO, and GOBC are compared in Fig. 1(a) where the stepwise changes in the functionalization process of the GO surface are clearly visible. For GO, the main characteristic absorbance peak appeared at 230 nm corresponding to the π–π* transitions of the C=C bonds of aromatic rings with a distinct shoulder peak near 290 nm for n–π* transition associated with the C=O bonds. The reported features are analogous to the spectrum of GO nanosheets prepared by following the Hummers' method.[39,40] In the spectrum of CGO, the shoulder disappeared while maintaining the prominent absorption peak at 230 nm with a slight increase in absorbance. These changes indicate the successful conversion of hydroxyl groups and epoxy groups of GO surface into carboxylic acid (COOH) groups.[41,42] Acrylate functionalization was introduced in CGO through the formation of C–N bonds which are indicated by the redshift of the peak at 230 nm to 256 nm observed in the spectrum of GOBC.[43,44] The preparation of GOBC from GO nanosheets was further confirmed from the FT-IR spectroscopic analysis of GO, CGO, and GOBC (Fig. 1(b)). In the spectrum of GOBC, the stretching vibrations of N–H, C=O, and C–N bonds of methacrylate groups were confirmed by the appearance of the peaks at 3360 cm^{-1}, 1728 cm^{-1}, and 1160 cm^{-1}, respectively. A peak that was observed at 1630 cm^{-1} attributed to the stretching vibrations of the HN–CO bond confirming the coupling of CGO and AEM.[45] A strong absorption band at 3450 cm^{-1} was observed for O–H groups and the peak at 1732 cm^{-1} corresponds to the C=O groups' band stretching of carboxylic acid. The peaks at 1220 cm^{-1} and 1620 cm^{-1} are attributed to the stretching vibration of C–O–C bonds of epoxy groups and aromatic C=C bonds, respectively. These observations suggest

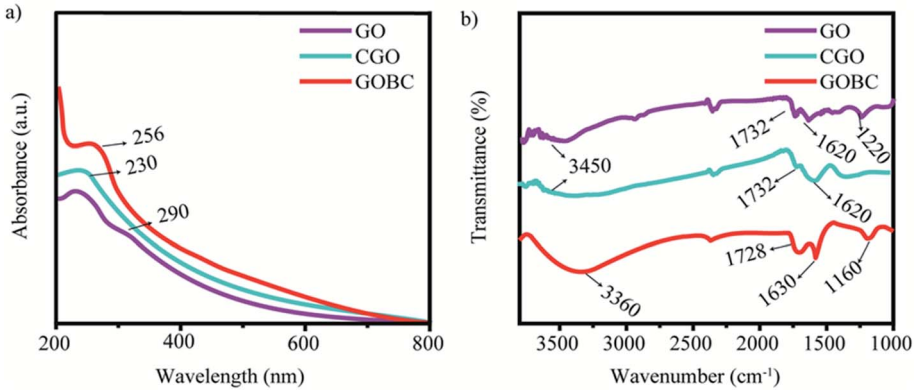

Fig. 1 Comparison of (a) UV-Vis spectra and (b) FT-IR spectra of GO, CGO, and GOBC.

that GOBC has been successfully prepared from GO by oxidation and acrylate functionalization. In GOBC, the C=C bond of an acrylate group can be used for covalent crosslinking with other monomers. In addition to that, the functional groups on the GOBC surface (O–H, COOH, and C–O–C) would be available for other bonding interactions such as hydrogen bonding, dipole–dipole interaction, electrostatic interaction, *etc.* These interactions are helpful for making attractive interactions in the dielectric water system of hydrogel networks.[46]

3.2 Mechanical properties of PAM nanocomposite hydrogels

The mechanical properties of the pure PAM hydrogel, PAM hydrogel with a conventional crosslinker, MBA, GO and PAM-GOBC hydrogels with different compositions of GOBC were characterized by tensile tests to study the effect of the crosslinkers. Fig. 2(a) shows the comparative stress–strain behavior of PAM hydrogels with different types and compositions of crosslinkers obtained from the tensile tests performed at the same velocity (100 mm min^{-1}). Young's modulus, toughness, and the tensile strength of the prepared hydrogels are shown in the bar chart (Fig. 2(b)). The summary of the data is also provided in ESI Table S1.† It was found that the mechanical properties are highly dependent on the type and compositions of the crosslinkers.

The Young's modulus, tensile strength, elongation at break, and toughness of PAM-GOBC-0.05% hydrogel are significantly higher than the PAM hydrogel prepared with the similar mass% of MBA crosslinker as shown in Fig. 2. It demonstrates the strong crosslinking ability of GOBC in PAM hydrogels. The Young's modulus and tensile strength of PAM-GOBC hydrogel are gradually improved by the increment in the composition of GOBC in the range of 0.01% to 0.05%. It provides strong evidence of covalent crosslinking inside the gel matrix. The reduction of elongation at break also supports the strong covalent crosslinking bond formation of GOBC. However, the enhancement of the overall toughness of the prepared PAM-GOBC hydrogel indicates strong viscoelastic energy dissipation from physical and chemical bonding. The PAM-GOBC hydrogels showed excellent mechanical toughness to endure high deformations in tension without obvious damage. The GOBC has been designed in such a way that it is capable of forming covalent bonds with the polymer matrix by methacrylate functional group in addition to the physical crosslinking

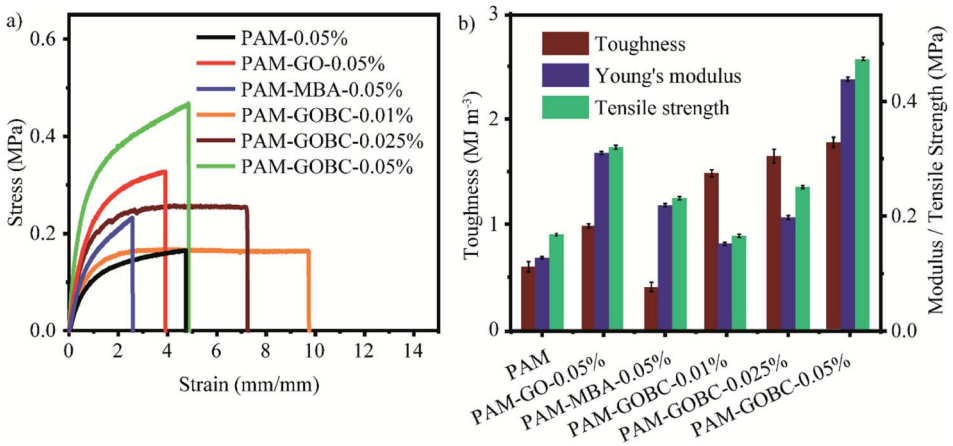

Fig. 2 (a) Comparison of stress–strain curves of PAM hydrogels with different crosslinkers obtained from the tensile tests performed at the same velocity of 100 mm min^{-1}. (b) Comparison of Young's modulus, tensile strength, and toughness of PAM hydrogels with different crosslinkers.

through dispersive interactions, hydrogen bonding, dipole–dipole interactions, and electrostatic interactions of the functional groups present over the surface GOBC. Among all these different types of interactions, covalent bonding is the dominant one that allowed PAM-GOBC hydrogel to exhibit remarkable tensile strength before breaking. The contribution of physical crosslinking from the GO surface can easily be understood when the stress–strain behavior of PAM-GO-0.05% and PAM-MBA-0.05% are compared. Both modulus and toughness of PAM hydrogel are improved by the presence of GO surfaces. A similar type of mechanism is also expected for PAM-GOBC hydrogels.

The parameters for the mechanical properties of PAM-GOBC are compared with other PAM hydrogels containing different crosslinkers. In the present work, the toughness for PAM-GOBC-0.05% hydrogel is found to be 1.775 MJ m^{-3} with a high modulus of 0.446 MPa. With a specially designed bi-functional silica nanoparticle (BF-Si NPs) 3D crosslinker with similar composition, the reported overall toughness of PAM-BF-Si NPs-0.05% hydrogel was only 0.655 MJ m^{-3} (ref. 48) which is three times lower than the value reported for PAM-GOBC. The 2D molybdenum disulfide (MoS_2) crosslinker in PAM showed a low toughness of 0.6 MJ m^{-3}.[48] The PAM hydrogels with chitosan-modified chitin nanocrystals (CNCs), and lignin nanoparticles (LNP) crosslinkers possessed maximum tensile strength of 0.09, and 0.110 Mpa[49,50] respectively which are lower than the observed maximum tensile strength of PAM-GOBC hydrogel, 0.473 MPa.

3.3 Swelling behavior of PAM-GOBC hydrogel

The swelling behavior of PAM hydrogels with different crosslinkers was studied at room temperature, and the changes in swelling kinetics are compared in Fig. 3. After immersing in DI water, the PAM-MBA-0.05% hydrogel showed a moderate water uptake over a period of 48 h. Similar swelling trends were also observed for the PAM-GOBC hydrogels. The swelling ratio of PAM-GOBC hydrogels increased sharply at the beginning but plateaued after a few hours. It suggests that the crosslinking ability of GOBC is good enough to inhibit the disintegration of hydrogels during water swelling. An increase of GOBC content from 0.01% to 0.05% in PAM hydrogels resulted in a decrease in the swelling capacity of hydrogels. The PAM-GOBC hydrogels with lower crosslinking concentrations are easily separated in water indicating the dominance of physical non-covalent interactions in the polymer matrices. On the other hand, the swelling ratio of PAM-GOBC-0.05% hydrogel is about 13 g g^{-1} (48 h), which is about two times lower than that of PAM-GOBC-0.01% hydrogel at the same swelling time. However, even after 48 h, all the PAA-GOBC hydrogels showed a very nominal level of changes of dimension and weight with time. This significantly reduced swelling tendency of PAM-GOBC-0.05% hydrogel suggests the presence of maximum covalent interaction inside the matrix. Therefore, the GOBC can modulate the dominance of covalent and non-covalent interactions in the gel matrix with the variation of its composition. Moreover, it was possible only due to the presence of a wide range of crosslinking sites with diverse nature of bonding in GOBC.

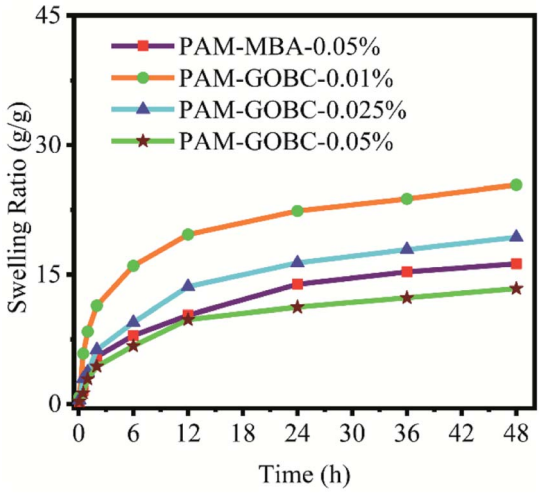

Fig. 3 The variation of the swelling ratio of different PAM hydrogels in water with immersion time.

3.4 Self-healing properties of PAM-GOBC hydrogel

The self-healing properties of PAM-GOBC hydrogels were analyzed to evaluate the efficiency of GOBC to recover its bonding. Rectangular-shaped PAM-GOBC hydrogel samples were cut into two pieces, and the cut sites were brought in contact immediately and kept in an airtight box for self-healing. The healed hydrogel samples were collected from the box after different time durations to study the change in self-healing capability with time by tensile tests. The tensile stress–strain behavior of PAM-GOBC-0.01%, PAM-GOBC-0.025%, PAM-GOBC-0.035%, and PAM-GOBC-0.05% hydrogels healed for different times are compared in Fig. 4(a)–(d) respectively. The healed hydrogels were not mechanically as tough as the original ones. It is no surprise due to the fact that the presence of both reversible bonds and irreversible covalent bonds is the source of the toughness in original PAM-GOBC hydrogels, whereas the healed interface contains only the reversible dynamic non-covalent bonds. However, for all cut PAM-GOBC hydrogels the stress–strain behavior improved with increasing contact time. The improvement is markedly prominent in PAM-GOBC-0.05% with the maximum concentration of GOBC. It showed maximum recovered modulus and toughness.

The cut boundaries of the PAM-GOBC hydrogels gradually disappeared with time demonstrating the real-time self-healing behavior. The images of PAM-GOBC-0.05% original, cut and healed (after 20 h) samples are shown in Fig. 5(a)–(c), respectively. The cut joint is almost unnoticeable in the healed hydrogel. The excellent healing capacity allows the healed hydrogel samples to be stretched (Fig. 5(d)), double twisted (Fig. 5(e)) or even bent (Fig. 5(f)) without causing noticeable damage.

The change in stress healing efficiency of PAM-GOBC hydrogels with time is plotted in Fig. 6(a). As the figure shows, the self-healing efficiency of hydrogels is strongly

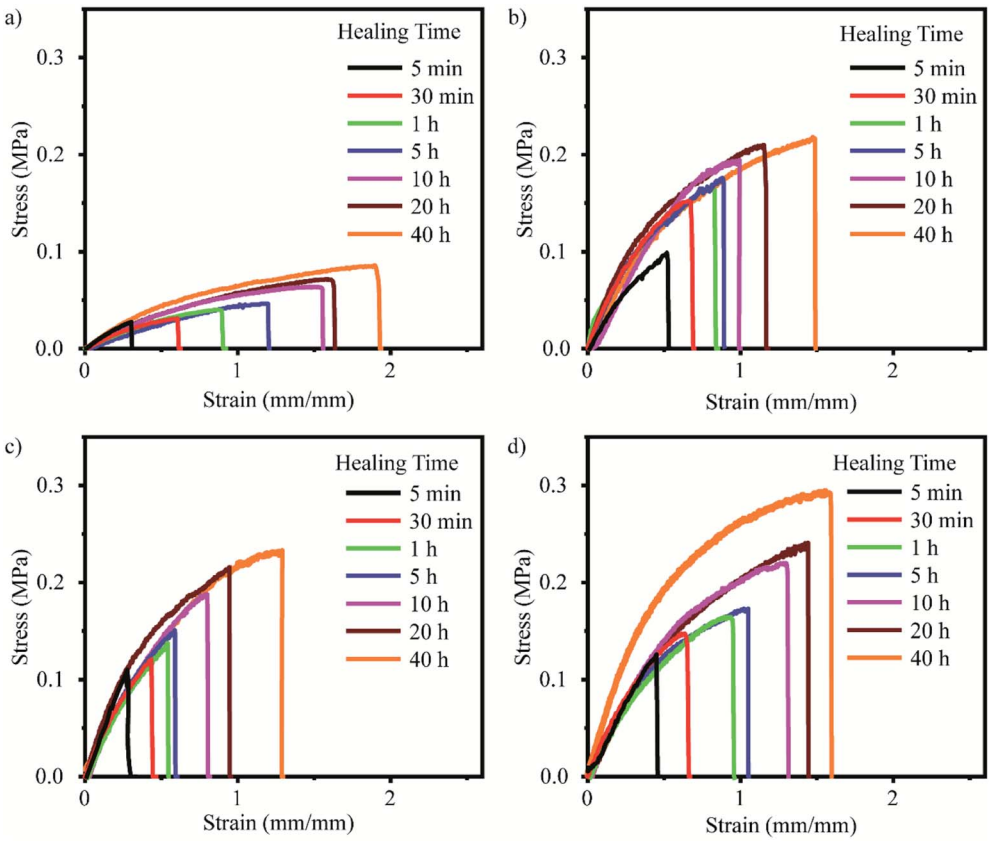

Fig. 4 Stress–strain curves of self-healed PAM hydrogel with (a) 0.01%, (b) 0.025%, (c) 0.035%, and (d) 0.05% GOBC.

dependent on the contact time of cut hydrogels as well as on the composition of GOBC. The self-healing efficiency improved noticeably as the composition of GOBC increased in the hydrogels. The PAM-GOBC-0.01%, PAM-GOBC-0.025%, PAM-GOBC-0.035%, and PAM-GOBC-0.05% hydrogels achieved maximum healing efficiency of 48%, 60%, 63%, and 70%, respectively, after 40 h. Whereas PAM-MBA-0.05% demonstrated no healing even after 40 h. For PAM-GOBC-0.05%, about 50% healing efficiency is achieved within 10 h contact time. To investigate the variation of self-healing efficiency with the mechanical properties of PAM-GOBC hydrogels, the stress-healing efficiency of PAM-GOBC hydrogels prepared with different concentrations of crosslinker was calculated at 40 h contact time and has been plotted against Young's modulus of the original samples in Fig. 6(b). It shows that the incorporation of GOBC in PAM hydrogels resulted in improved mechanical and self-healing properties, simultaneously. Initially, up to 0.2 MPa, the self-healing efficiency improved significantly with the enhancement of modulus. Here, increase in amount of GOBC, increased the number of covalent bonds contributing in the modulus and additionally increased the number of reversible hydrogen bonds contributing in the enhanced bond

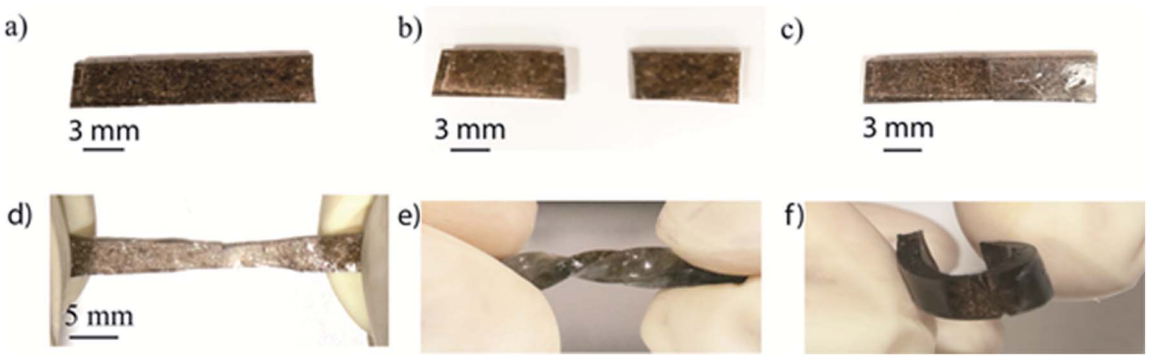

Fig. 5 Real-time images of PAM-GOBC-0.05%; (a) fresh sample, (b) cut sample, (c) healed sample after 20 h, (d) stretched healed sample, (e) a double twist of the healed sample, and (f) bent healed sample.

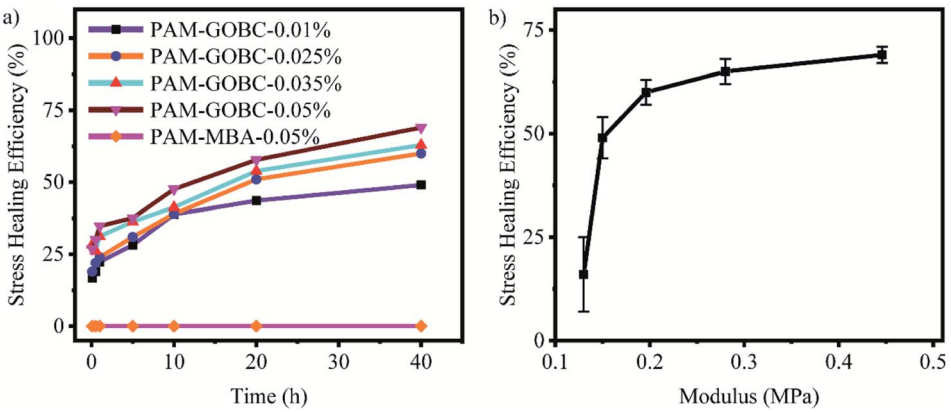

Fig. 6 (a) Variation of stress healing efficiency of PAM hydrogels prepared with different crosslinkers. (b) A plot of the self-healing efficiency of different PAM-GOBC hydrogels with the corresponding Young's modulus of the original samples.

reforming capability. In the range of modulus 0.2 to 0.45 MPa, the self-healing efficiency reached maximum values and increased moderately by the enhancement of modulus. It is due to the presence of saturated amounts of reversible contact sites at very high modulus in high concentration of GOBC. This kind of trend in modulus and self-healing efficiency is unique compared to most of the reported works on hydrogel self-healing efficiency.

Most studies support the Dahlquist criterion that the self-healing efficiency decreases with the increase in modulus, and high self-healing efficiency is difficult to obtain in high modulus hydrogels especially over 0.1 MPa.[31,51] For a PAM-based graphene oxide/hydrophobically associated composite hydrogel, Cui *et al.* showed that a high self-healing efficiency of 53% could be achieved with a low modulus of 0.065 MPa.[52] A moderate 40% self-healing efficiency was observed for a relatively higher modulus, 0.0106 MPa agar/PAM hydrogel.[43] However, according to a study reported by Zhao *et al.*, for a very high modulus (0.350 MPa), sodium alginate/PAM hydrogel only 35% self-healing efficiency at room temperature was achieved.[53] Ihsan *et al.* prepared a polyampholyte hydrogel and reported that the increment of the amount of chemical crosslinker, MBA from 0 to 4% in the hydrogel led to increase in the elastic modulus from 0.072 to 0.4 MPa which resulted in a significant decrease in self-healing efficiency from 92.11% to 2.76%.[31] In aniline/phytic acid hydrogel, high tough gel (7.85 kPa) was obtained in high concentration (0.15 mol%) of aniline filler.[54] However, the self-healing efficiency was 66% even after 72 h. Limited self-healing behavior was also observed for high modulus hydrogels in the work described by Pan *et al.*[55] The increase in GO content as crosslinker in poly(acrylamide-*co*-2-(dimethylamino) ethylacrylatemethochloride) resulted in a hydrogel with enhanced mechanical properties, but compromise in the self-healing ability.

In this study, a maximum of 70% self-healing efficiency was successfully achieved for PAM-GOBC hydrogel having a high modulus of 0.446 MPa. It suggests the unique contribution of GOBC with the increased concentration improved both modulus and self-healing efficiency. A new strategy was introduced in this work for incorporating GO in the form of a crosslinker GOBC, capable of providing both physical and chemical bonds simultaneously. Most of the conventional crosslinkers provide only covalent bonds while the incorporation of ionic or hydrogen bonds reduces the amount of permanent covalent bond. The physical and chemical bonds provided by GOBC give rise to the simultaneous improvement of mechanical and self-healing properties of the prepared hydrogel similar facts were observed in the report of Shanshan *et al.*, where strong polyampholyte gels with high self-healing efficiency of 70% was obtained by introducing large number of physical bonding sites using a third monomer 2-ureidoethyl methacrylate.[56] In this work, we showed that the unusual combination of self-healing property and strong mechanical properties in the same hydrogel might be possible by using a GOBC crosslinker. The increase in the amount of GOBC in hydrogels simultaneously increases the number of physical and chemical crosslinking sites. The chemical crosslinker with covalent bonds is considered as strong bonds that hold the material leading to better mechanical strength, whereas a large number of physical crosslinking sites with hydrogen bonds form weaker bonds that retain chain mobility for better bond reformation and greater self-healing efficiency. The mobility of the polymer networks and the reformation of the reversible bonding interactions in the polymer matrix during the contact of two cut pieces of hydrogels cause the disappearances of the crack between the separate parts as time goes. In the case of PAM-GOBC, the cracks almost disappeared after 20 h of contact time. The self-healing mechanism of PAM-GOBC hydrogel is presented schematically in Fig. 7. The healing is attributed to the adsorption of polymeric networks of hydrogels over the GOBC surface. As we discussed, the GOBC surface contains a large number of hydrophilic groups such as $-NH_2$, –OH, and –COOH groups. The presence of these dominant hydrophilic groups, in the healing response of PAM-GOBC hydrogels, the polymer networks are easily adsorbed over the GOBC surface *via* hydrogen bonding and electrostatic interaction.[47] The hydrophobic groups on the GOBC surface are also well capable of forming reversible dynamic noncovalent bonds like van der

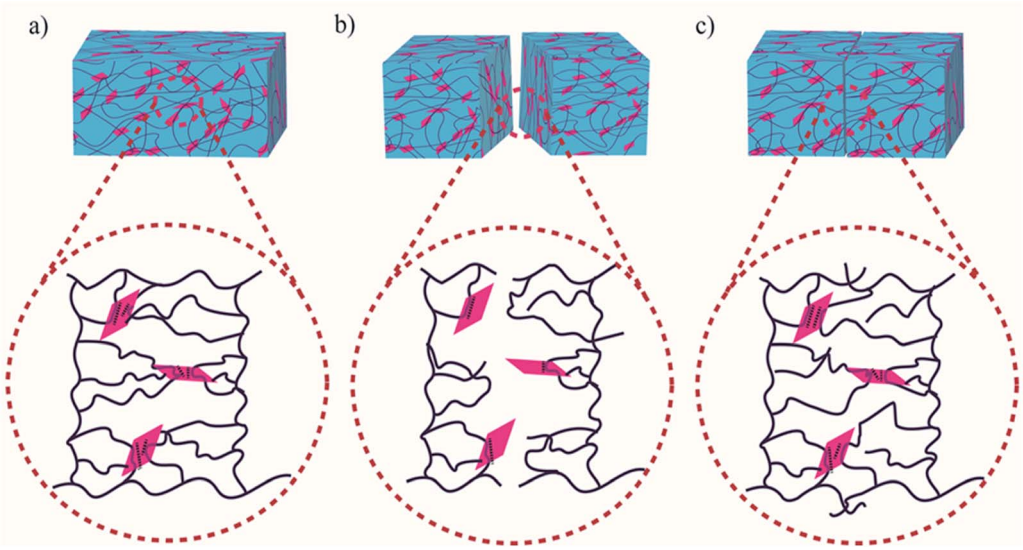

Fig. 7 Self-healing mechanism of PAA-GOBC composite hydrogel; (a) fresh sample, (b) cut sample, and (c) healed sample.

Waals and π–π stacking with the polymer networks at the cutting interfaces even in presence of water.[57,58] These reversible bonds contributed effectively to the rebonding of the polymeric networks, recovering the damage of PAM-GOBC hydrogels without any external stimuli. A self-healing material is required to possess a sufficient number of active sites for efficient recovery. The GOBC crosslinker with an abundance of non-specific crosslinking sites effectively contributed to the self-healing efficiency of hydrogels which dictate its universal character.

3.5 Self-healing behavior of PAA-GOBC hydrogel

The self-healing behavior of a GOBC crosslinked PAA hydrogel was also investigated to explore the universal applicability of GOBC for forming self-healable hydrogels with different polymers. A PAA-GOBC-0.05% hydrogel was prepared and its self-healing behavior was investigated. The stress–strain behavior of the original and healed PAA-GOBC-0.05% hydrogels are compared in Fig. 8. It can be observed that the GOBC crosslinker is capable of healing the fractured surface of PAA-GOBC as well. The healed sample was capable of achieving remarkable tensile strength with a moderate stretchability before the fracture. PAA-GOBC demonstrated almost 60% of stress healing efficiency within 40 h contact time.

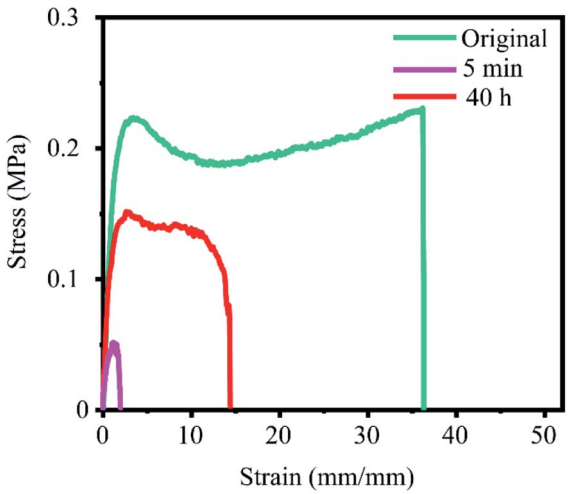

Fig. 8 Stress–strain curves of self-healing ability for PAA-GOBC-0.05% after 5 min and 40 h healing time.

4. Conclusions

A special type of GOBC has been successfully prepared by oxidation and vinyl functionalization of GO. The GOBC demonstrated strong crosslinking ability with conventional PAM and PAA hydrogels. The presence of both covalent and non-covalent interactions of GOBC helps to restrict the disintegration of polymer-GOBC hydrogels in the dielectric water system during swelling, and also enhances the mechanical properties. The mechanical properties such as tensile strength, Young's modulus, and toughness are significantly improved by the incorporation of GOBC without compromising self-healing efficiency. A maximum of 70% healing efficiency is achieved in PAM-GOBC hydrogel with 0.05% crosslinker (mass% with respect to monomer) at high modulus and toughness of the hydrogel. A similar improvement in the mechanical and self-healing properties of PAA-GOBC supports the universality of GOBC as an effective crosslinker. The conventional non-healable hydrogels are easily converted into highly self-healable hydrogels by utilizing GOBC. Therefore, this crosslinker-based approach for simultaneous improvement of mechanical property and self-healing capability is expected to widen the scopes of hydrogel applications.

Conflicts of interest

There are no conflicts to declare.

Acknowledgements

The research was conducted using the instrumental support of the Bangladesh University of Engineering and Technology (BUET) purchased under different projects approved by the Committee for Advanced Studies and Research (CASR) – BUET. The authors acknowledge the support of this research, from a project approved by the Ministry of Education, Government of the People's Republic of Bangladesh (PS20191001).

References

1 K. Cui, T. L. Sun, X. Liang, K. Nakajima, Y. N. Ye, L. Chen, T. Kurokawa and J. P. Gong, Multiscale Energy Dissipation Mechanism in Tough and Self-Healing Hydrogels, *Phys. Rev. Lett.*, 2018, **121**(18), 185501, DOI: 10.1103/PhysRevLett.121.185501.

2 F. Luo, T. L. Sun, T. Nakajima, T. Kurokawa, Y. Zhao, K. Sato, A. B. Ihsan, X. Li, H. Guo and J. P. Gong, Oppositely charged polyelectrolytes form tough, self-healing, and rebuildable hydrogels, *Adv. Mater.*, 2015, **27**(17), 2722–2727, DOI: 10.1002/adma.201500140.

3 K. Cui, Y. N. Ye, T. L. Sun, C. Yu, X. Li, T. Kurokawa and J. P. Gong, Phase Separation Behavior in Tough and Self-Healing Polyampholyte Hydrogels, *Macromolecules*, 2020, **53**(13), 5116–5126, DOI: 10.1021/acs.macromol.0c00577.

4 M. A. Hossain, C. K. Roy, S. D. Sarkar, H. Roy, A. H. Howlader and S. H. Firoz, Improvement of the strength of poly(acrylic acid) hydrogels by the incorporation of functionally modified nanocrystalline Cellulose, *Mater. Adv.*, 2020, **1**(6), 2107–2116, DOI: 10.1039/d0ma00478b.

5 X. Li, L. Kong and G. Gao, A bio-inspired self-recoverable polyampholyte hydrogel with low temperature sensing, *J. Mater. Chem. B*, 2021, **9**(8), 2010–2015, DOI: 10.1039/D0TB02895A.

6 M. J. Hossen, S. D. Sarkar, M. M. Uddin, C. K. Roy and M. S. Azam, Mussel-Inspired Adhesive Nano-Filler for Strengthening Polyacrylamide Hydrogel, *ChemistrySelect*, 2020, **5**(29), 8906–8914, DOI: 10.1002/slct.202001632.

7 A. K. Patterson and D. K. Smith, Two-component supramolecular hydrogel for controlled drug release, *Chem. Commun.*, 2020, **56**(75), 11046–11049, DOI: 10.1039/d0cc03962d.

8 F. Ma, Y. Yan, Z. Yu, Y. Wu and X. Liu, Freestanding flexible molecularly imprinted nanocomposite membranes for selective separation applications: an imitated core–shell PEI@SiO_2-based MIM design, *New J. Chem.*, 2020, **44**(44), 19091–19102, DOI: 10.1039/d0nj03489d.

9 J. Chen, M. Li, W. Hong, Y. Xia, J. Lin and X. Chen, Bioinspired interconnected hydrogel capsules for enhanced catalysis, *RSC Adv.*, 2018, **8**(65), 37050–37056, DOI: 10.1039/c8ra07037g.

10 F. Versluis, D. M. van Elsland, S. Mytnyk, D. L. Perrier, F. Trausel, J. M. Poolman, C. Maity, V. A. le Sage, S. I. van Kasteren, J. H. van Esch and R. Eelkema, Negatively Charged Lipid Membranes Catalyze Supramolecular Hydrogel Formation, *J. Am. Chem. Soc.*, 2016, **138**(28), 8670–8673, DOI: 10.1021/jacs.6b03853.

11 K. Y. Lee and D. J. Mooney, Hydrogels for tissue engineering, *Chem. Rev.*, 2001, **101**(7), 1869–1880, DOI: 10.1021/cr000108x.

12 Y. Zhang, B. Yang, X. Zhang, L. Xu, L. Tao, S. Li and Y. Wei, A magnetic self-healing hydrogel, *Chem. Commun.*, 2012, **48**(74), 9305–9307, DOI: 10.1039/c2cc34745h.

13 D. Seliktar, Designing cell-compatible hydrogels for biomedical applications, *Science*, 2012, **336**(6085), 1124–1128, DOI: 10.1126/science.1214804.

14 R. K. Das, V. Gocheva, R. Hammink, O. F. Zouani and A. E. Rowan, Stress-stiffening-mediated stem-cell commitment switch in soft responsive hydrogels, *Nat. Commun.*, 2016, **15**(3), 318–325, DOI: 10.1038/nmat4483.

15 H. Qin, T. Zhang, N. Li, H. P. Cong and S. H. Yu, Anisotropic and self-healing hydrogels with multi-responsive actuating capability, *Nat. Commun.*, 2019, **10**(1), 2202, DOI: 10.1038/s41467-019-10243-8.

16 J. Wu, P. Li, C. Dong, H. Jiang, X. Bin, X. Gao, M. Qin, W. Wang, C. Bin and Y. Cao, Rationally designed synthetic protein hydrogels with predictable mechanical properties, *Nat. Commun.*, 2018, **9**(1), 620, DOI: 10.1038/s41467-018-02917-6.

17 S. Tepic, T. Macirowski and R. W. Mann, Mechanical properties of articular cartilage elucidated by osmotic loading and ultrasound, *Proc. Natl. Acad. Sci. U. S. A.*, 1983, **80**(11), 3331–3333, DOI: 10.1073/pnas.80.11.3331.

18 W. Wang, R. Narain and H. Zeng, Rational Design of Self-Healing Tough Hydrogels: A Mini Review, *Front. Chem.*, 2018, **6**, 497, DOI: 10.3389/fchem.2018.00497.

19 D. L. Taylor and M. In Het Panhuis, Self-Healing Hydrogels, *J. Adv. Mater.*, 2016, **28**(41), 9060–9093, DOI: 10.1002/adma.201601613.

20 P. Heidarian, A. Z. Kouzani, A. Kaynak, A. Zolfagharian and H. Yousefi, Dynamic Mussel-Inspired Chitin Nanocomposite Hydrogels for Wearable Strain Sensors, *Polymers*, 2020, **12**(6), 1416, DOI: 10.3390/polym12061416.

21 H. Qin, T. Zhang, H.-N. Li, H.-P. Cong, M. Antonietti and S.-H. Yu, Dynamic Au-Thiolate Interaction Induced Rapid Self-Healing Nanocomposite Hydrogels with Remarkable Mechanical Behaviors, *Chem*, 2017, **3**(4), 691–705, DOI: 10.1016/j.chempr.2017.07.017.

22 T. L. Sun, F. Luo, W. Hong, K. Cui, Y. Huang, H. J. Zhang, D. R. King, T. Kurokawa, T. Nakajima and J. P. Gong, Bulk Energy Dissipation Mechanism for the Fracture of Tough and Self-Healing Hydrogels, *Macromolecules*, 2017, **50**(7), 2923–2931, DOI: 10.1021/acs.macromol.7b00162.

23 H. Rammal, A. GhavamiNejad, A. Erdem, R. Mbeleck, M. Nematollahi, S. Emir Diltemiz, H. Alem, M. A. Darabi, Y. N. Ertas, E. J. Caterson and N. Ashammakhi, Advances in biomedical applications of self-healing hydrogels, *Mater. Chem.*, 2021, **5**(12), 4368–4400, DOI: 10.1039/d0qm01099e.

24 I. Hussain, S. M. Sayed, S. Liu, F. Yao, O. Oderinde and G. Fu, Hydroxyethyl cellulose-based self-healing hydrogels with enhanced mechanical properties *via* metal–ligand bond

interactions, *Eur. Polym. J.*, 2018, **100**, 219–227, DOI: 10.1016/j.eurpolymj.2018.01.002.

25 L. Cai, S. Liu, J. Guo and Y. G. Jia, Polypeptide-based self-healing hydrogels: Design and biomedical applications, *Acta Biomater.*, 2020, **113**, 84–100, DOI: 10.1016/j.actbio.2020.07.001.

26 Y. Deng, I. Hussain, M. Kang, K. Li, F. Yao, S. Liu and G. Fu, Self-recoverable and mechanical-reinforced hydrogel based on hydrophobic interaction with self-healable and conductive properties, *Chem. Eng. J.*, 2018, **353**, 900–910, DOI: 10.1016/j.cej.2018.07.187.

27 M. Zhong, X. Y. Liu, F. K. Shi, L. Q. Zhang, X. P. Wang, A. G. Cheetham, H. Cui and X. M. Xie, Self-healable, tough and highly stretchable ionic nanocomposite physical hydrogels, *Soft Matter*, 2015, **11**(21), 4235–4241, DOI: 10.1039/c5sm00493d.

28 Q. Yang, P. Wang, C. Zhao, W. Wang, J. Yang and Q. Liu, Light-Switchable Self-Healing Hydrogel Based on Host–Guest Macro-Crosslinking, *Macromol. Rapid Commun.*, 2017, **38**(6), 1600741, DOI: 10.1002/marc.201600741.

29 U. Gulyuz and O. Okay, Self-healing polyacrylic acid hydrogels, *Soft Matter*, 2013, **9**(43), 10287–10293, DOI: 10.1039/c3sm52015c.

30 T. L. Sun, F. Luo, T. Kurokawa, S. N. Karobi, T. Nakajima and J. P. Gong, Molecular structure of self-healing polyampholyte hydrogels analyzed from tensile behaviors, *Soft Matter*, 2015, **11**(48), 9355–9366, DOI: 10.1039/c5sm01423a.

31 A. B. Ihsan, T. L. Sun, T. Kurokawa, S. N. Karobi, T. Nakajima, T. Nonoyama, C. K. Roy, F. Luo and J. P. Gong, Self-Healing Behaviors of Tough Polyampholyte Hydrogels, *Macromolecules*, 2016, **49**(11), 4245–4252, DOI: 10.1021/acs.macromol.6b00437.

32 H. Fan, J. Wang and Z. Jin, Tough, Swelling-Resistant, Self-Healing, and Adhesive Dual-Cross-Linked Hydrogels Based on Polymer–Tannic Acid Multiple Hydrogen Bonds, *Macromolecules*, 2018, **51**(5), 1696–1705, DOI: 10.1021/acs.macromol.7b02653.

33 M. I. Sujan, S. D. Sarkar, C. K. Roy, M. Ferdous, A. Goswami, M. A. Gafur and M. S. Azam, Graphene oxide crosslinker for the enhancement of mechanical properties of polylactic acid, *J. Polym. Sci.*, 2021, **59**(11), 1043–1054, DOI: 10.1002/pol.20210029.

34 S. D. Sarkar, M. M. Uddin, C. K. Roy, M. J. Hossen, M. I. Sujan and M. S. Azam, Mechanically tough and highly stretchable poly(acrylic acid) hydrogel cross-linked by 2D graphene oxide, *RSC Adv.*, 2020, **10**(18), 10949–10958, DOI: 10.1039/d0ra00678e.

35 W. S. Hummers Jr and R. E. Offeman, Preparation of graphitic oxide, *J. Am. Chem. Soc.*, 1958, **80**(6), 1339, DOI: 10.1021/ja01539a017.

36 N. Zhang, R. Li, L. Zhang, H. Chen, W. Wang, Y. Liu, T. Wu, X. Wang, W. Wang and Y. J. S. M. Li, Actuator materials based on graphene oxide/polyacrylamide composite hydrogels prepared by *in situ* polymerization, *Soft Matter*, 2011, **7**(16), 7231–7239, DOI: 10.1039/C1SM05498H.

37 J. Meid, F. Dierkes, J. Cui, R. Messing, A. J. Crosby, A. Schmidt and W. Richtering, Mechanical properties of temperature sensitive microgel/polyacrylamide composite hydrogels-from soft to hard fillers, *Soft Matter*, 2012, **8**(15), 4254–4263, DOI: 10.1039/c2sm06868k.

38 B. Ramaraj and G. Radhakrishnan, Interpenetrating hydrogel networks based on gelatin and polyacrylamide: Synthesis, swelling, and drug release analysis. Journal of Applied, *Polym. Sci.*, 1994, **52**(7), 837–846, DOI: 10.1002/app.1994.070520701.

39 J.-Y. Hong and J. Jang, Highly stable, concentrated dispersions of graphene oxide sheets and their electro-responsive characteristics, *Soft Matter*, 2012, **8**(28), 7348–7350, DOI: 10.1039/c2sm25865j.

40 D. C. Marcano, D. V. Kosynkin, J. M. Berlin, A. Sinitskii, Z. Sun, A. Slesarev, L. B. Alemany, W. Lu and J. M. Tour, Improved Synthesis of Graphene Oxide, *ACS Nano*, 2010, **4**(8), 4806–4814, DOI: 10.1021/nn1006368.

41 H. Zhang, R. Huang, H. Cang, Z. Cai and B. Sun, Graphene oxide-coumarin derivative conjugate as activatable nanoprobe for intracellular imaging with one- or two-photon excitation, *J. Mater. Chem. B*, 2014, **2**(12), 1742–1750, DOI: 10.1039/c3tb21656j.

42 Z. Zhu, L. Ma, M. Su, D. Liu and Z. Wang, Preparation and application of thionin-bridged graphene-gold nanoparticle nanohybrids, *J. Mater. Chem. B*, 2013, **1**(10), 1432–1438, DOI: 10.1039/c2tb00117a.

43 X. Yan, Q. Chen, L. Zhu, H. Chen, D. Wei, F. Chen, Z. Tang, J. Yang and J. Zheng, High strength and self-healable gelatin/polyacrylamide double network hydrogels, *J. Mater. Chem. B*, 2017, **5**(37), 7683–7691, DOI: 10.1039/c7tb01780d.

44 W. Zhang, J. Ma, D. Gao, Y. Zhou, C. Li, J. Zha and J. Zhang, Preparation of amino-functionalized graphene oxide by Hoffman rearrangement and its performances on polyacrylate coating latex, *Prog. Org. Coat.*, 2016, **94**, 9–17, DOI: 10.1016/j.porgcoat.2016.01.013.

45 H. Tetsuka, R. Asahi, A. Nagoya, K. Okamoto, I. Tajima, R. Ohta and A. J. A. M. Okamoto, Optically tunable amino-functionalized graphene quantum dots, *Adv. Mater.*, 2012, **24**(39), 5333–5338, DOI: 10.1002/adma.201201930.

46 J. Zhou, S. Lin, H. Zeng, J. Liu, B. Li, Y. Xu, X. Zhao and G. Chen, Dynamic intermolecular interactions through hydrogen bonding of water promote heat conduction in hydrogels, *Mater. Horiz.*, 2020, **7**(11), 2936–2943, DOI: 10.1039/d0mh00735h.

47 M. I. Sujan, S. D. Sarkar, S. Sultana, L. Bushra, R. Tareq, C. K. Roy and M. S. Azam, Bi-functional silica nanoparticles for simultaneous enhancement of mechanical strength and swelling capacity of hydrogels, *RSC Adv.*, 2020, **10**(11), 6213–6222, DOI: 10.1039/c9ra09528d.

48 K. M. Lee, Y. Oh, H. Yoon, M. Chang and H. Kim, Multifunctional Role of MoS_2 in Preparation of Composite Hydrogels: Radical Initiation and Cross-Linking, *ACS Appl. Mater. Interfaces*, 2020, **12**(7), 8642–8649, DOI: 10.1021/acsami.9b19567.

49 M. Liu, J. Huang, B. Luo and C. Zhou, Tough and highly stretchable polyacrylamide nanocomposite hydrogels with chitin nanocrystals, *Int. J. Biol. Macromol.*, 2015, **78**, 23–31, DOI: 10.1016/j.ijbiomac.2015.03.059.

50 Y. Chen, K. Zheng, L. Niu, Y. Zhang, Y. Liu, C. Wang and F. Chu, Highly mechanical properties nanocomposite hydrogels with biorenewable lignin nanoparticles. International Journal of Biological, *Macromolecules*, 2019, **128**, 414–420, DOI: 10.1016/j.ijbiomac.2019.01.099.

51 S. S. Heddleson, D. D. Hamann and D. R. Lineback, The Dahlquist criterion: applicability of a rheological criterion to the loss of pressure-sensitive tack in flour-water dough, *Cereal Chem.*, 1993, **70**(6), 744–748, DOI: https://pascal-francis.inist.fr/vibad/index.php?action=getRecordDetail&idt=4001275.

52 W. Cui, J. Ji, Y.-F. Cai, H. Li and R. Ran, Robust, anti-fatigue, and self-healing graphene oxide/hydrophobically associated composite hydrogels and their use as recyclable adsorbents for dye wastewater treatment, *J. Mater. Chem. A*, 2015, **3**(33), 17445–17458, DOI: 10.1039/c5ta04470g.

53 D. Zhao, M. Feng, L. Zhang, B. He, X. Chen and J. Sun, Facile synthesis of self-healing and layered sodium alginate/polyacrylamide hydrogel promoted by dynamic hydrogen bond, *Carbohydr. Polym.*, 2021, **256**, 117580, DOI: 10.1016/j.carbpol.2020.117580.

54 G. Su, S. Yin, Y. Guo, F. Zhao, Q. Guo, X. Zhang, T. Zhou and G. Yu, Balancing the mechanical, electronic, and self-healing properties in conductive self-healing hydrogel for wearable sensor applications, *Mater. Horiz.*, 2021, **8**, 1795–1804, DOI: 10.1039/d1mh00085c.

55 C. Pan, L. Liu, Q. Chen, Q. Zhang and G. Guo, Tough, Stretchable, Compressive Novel Polymer/Graphene Oxide Nanocomposite Hydrogels with Excellent Self-Healing Performance, *ACS Appl. Mater. Interfaces*, 2017, **9**(43), 38052–38061, DOI: 10.1021/acsami.7b12932.

56 S. Wu, Z. Shao, H. Xie, T. Xiang and S. Zhou, Salt-mediated triple shape-memory ionic conductive polyampholyte hydrogel for wearable flexible electronics, *J. Mater. Chem. A*, 2021, **9**, 1048–1061, DOI: 10.1039/d0ta08664a.

57 P. Ren, J. Li, L. Zhao, A. Wang, M. Wang, J. Li, H. Jian, X. Li, X. Yan and S. Bai, Dipeptide Self-assembled Hydrogels with Shear-Thinning and Instantaneous Self-healing Properties Determined by Peptide Sequences, *ACS Appl. Mater. Interfaces*, 2020, **12**(19), 21433–21440, DOI: 10.1021/acsami.0c03038.

58 J. Zhang, B. Zhang, Q. Chen, B. Zhang and J. Song, Hofmeister Anion-Induced Tunable Rheology of Self-Healing Supramolecular Hydrogels, *Nanoscale Res. Lett.*, 2019, **14**(1), 5, DOI: 10.1186/s11671-018-2823-8.